

STAR FORMATION ACTIVITY OF BARRED SPIRAL GALAXIES

EUNBIN KIM¹, HO SEONG HWANG², HAEUN CHUNG^{3,4}, GWANG-HO LEE³, CHANGBOM PARK⁴, BERNARDO CERVANTES SODI⁵,
SUNGSOO S. KIM^{1,6}

Last updated: March 7, 2018

ABSTRACT

We study the star formation activity of nearby galaxies with bars using a sample of late-type galaxies at $0.02 \leq z \leq 0.05489$ and $M_r < -19.5$ from the Sloan Digital Sky Survey. We compare the physical properties of strongly and weakly barred galaxies with those of non-barred galaxies that have stellar mass and redshift distributions similar to barred galaxies. We find that the star formation activity of strongly barred galaxies probed by starburstiness, $g - r$, $\text{NUV} - r$, and mid-infrared [3.4]–[12] colors is, on average, lower than that of non-barred galaxies. However, weakly barred galaxies do not show such a difference between barred and non-barred galaxies. The amounts of atomic and molecular gas in strongly barred galaxies are smaller than those of non-barred galaxies, and the gas metallicity is higher in strongly barred galaxies than in non-barred galaxies. The gas properties of weakly barred galaxies again show no difference from those of non-barred galaxies. We stack the optical spectra of barred and non-barred galaxies in several mass bins and fit to the stacked spectra with a spectral fitting code, STARLIGHT. We find no significant difference in stellar populations between barred and non-barred galaxies for both strongly and weakly barred galaxies. Our results are consistent with the idea that the star formation activity of barred galaxies is enhanced in the past along with significant gas consumption, and is currently lower than or similar to that of non-barred galaxies. The past star formation enhancement depends on the strength of bars.

Keywords: galaxies: evolution – galaxies: formation – galaxies: ISM – galaxies: spiral – galaxies: star formation – galaxies: structure

1. INTRODUCTION

Star formation activity of galaxies is strongly affected by both internal and external physical processes. In the early universe, galaxy evolution is primarily determined by external effects that include hierarchical clustering and merging. Then, galaxy evolution becomes mainly secular, which is a rearrangement of energy and mass by non-axisymmetric galactic inner structures (Kormendy & Kennicutt 2004). The non-axisymmetric potential in galaxies can be driven by bars or ovals, which can cause the gas to lose angular momentum and to infall into a central region of galaxies from galactic disks. The gas accumulated in the galactic center becomes fuels for the central star formation (Athanasoula 1992).

Early studies showed that bars can play such a role in transporting gas into the galactic center. When a galaxy contains a bar in the central region, gas far from resonances tends to settle on periodic orbits including x_1 orbits that are elongated along the major axis of bars (Contopoulos & Papayannopoulos 1980; Binney et al. 1991; Morris & Serabyn 1996). The gas

then goes through shocks, flows inwards by losing angular momentum, and moves to the x_2 orbits elongated along the minor axis. The gas finally settles into stable orbits, which are close to the position of the inner Lindblad resonance (ILR) of the bar (Simkin et al. 1980; Combes & Gerin 1985). Because the gas accumulated in the central region is used for fuel of central star formation, the enhanced star formation activity in the central region could be a good indicator of recent gas inflow into the center (Knapen et al. 1995). Many numerical simulations indeed demonstrated that the star formation activity can be enhanced in central regions of galaxies when there are galactic bars (Shlosman et al. 1990; Athanassoula 1994; Combes 2001; Kim et al. 2011, 2012; Seo & Kim 2013; Shin et al. 2017).

Observations also showed enhanced star formation activity in central regions of barred galaxies. For example, Heckman (1980) found that recent star formation activity is more frequently observed in barred galaxies than in non-barred galaxies. The different star formation activity between barred and non-barred galaxies is also supported by multiwavelength observations (Hawarden et al. 1986; Devereux 1987; Himmel et al. 1990; Regen et al. 2006; Wang et al. 2012; Lin et al. 2017). The effects of bars tend to be stronger for the galaxies with earlier morphological types (Ho et al. 1997; Oh et al. 2012).

On the other hand, some observations found no increase in star formation activity in barred galaxies compared to non-barred galaxies (Pompea & Rieke 1990; Martinet & Friedli 1997; Chapelon et al. 1999; Cheung et al. 2013; Willett et al. 2015). Similarly, the amount of gas that is fuel for star formation is not

¹ School of Space Research, Kyung Hee University, Yongin, Gyeonggi 17104, Korea; ebkim@khu.ac.kr

² Quantum Universe Center, Korea Institute for Advanced Study, 85 Hoegiro, Dongdaemun-gu, Seoul 02455, Korea

³ Astronomy Program, Department of Physics and Astronomy, Seoul National University, 1 Gwanak-ro, Gwanak-gu, Seoul 08826, Korea

⁴ School of Physics, Korea Institute for Advanced Study, 85 Hoegiro, Dongdaemun-gu, Seoul 02455, Korea

⁵ Instituto de Radioastronomía y Astrofísica, Universidad Nacional Autónoma de México, Campus Morelia, A.P. 3-72, C.P. 58089 Michoacán, México

⁶ Department of Astronomy & Space Science, Kyung Hee University, Yongin, Gyeonggi 17104, Korea

larger in barred galaxies than in non-barred galaxies; the bar fraction decreases with increasing HI gas fraction of galaxies (Masters et al. 2012; Cervantes Sodi 2017). Saintonge et al. (2012) also suggested that bar instabilities do not significantly affect the star formation budget for local galaxies.

The complicated situation is not much different for the role of bars in triggering nuclear activity of galaxies. Oh et al. (2012) found that the effects of bars on the activity in galactic nuclei are stronger in bluer galaxies than in redder galaxies. However, Lee et al. (2012b) showed that the nuclear activity of barred galaxies does not differ from that of non-barred galaxies once the physical properties of host galaxies are well matched (see also Cisternas et al. 2013; Cheung et al. 2015).

To better understand the role of galactic bars in triggering star formation activity, we compare various physical properties of barred galaxies with those of carefully selected control sample of non-barred galaxies. The various physical parameters representing the star formation activity include starburstiness (a measure of the excess in specific star formation rate of a galaxy compared to the specific star formation rate of a main sequence star-forming galaxy with the same mass, Elbaz et al. 2011), multiwavelength photometric data including ultraviolet (UV) and mid-infrared, the amounts of atomic and molecular gas, and the gas metallicity. We compare the star formation activity not only between barred and non-barred galaxies, but also between strongly and weakly barred galaxies. We also fit to the optical spectra with STARLIGHT to make a detailed comparison of the stellar populations between barred and non-barred galaxies.

Section 2 describes the sample of barred galaxies and its control sample, and explains the observational data we use. We compare the star formation activity between barred and non-barred galaxies in Section 3. We discuss the results and conclude in Sections 4 and 5, respectively. Throughout, we adopt flat Λ cold dark matter cosmological parameters: $H_0 = 70 \text{ km s}^{-1} \text{ Mpc}^{-1}$, $\Omega_\Lambda = 0.7$, and $\Omega_m = 0.3$.

2. DATA

2.1. Samples of Galaxies with and without Bars

We use the samples of barred and non-barred galaxies described in Lee et al. (2012a), which were constructed from a volume-limited sample of 33,391 galaxies at $0.02 \leq z \leq 0.05489$ and $M_r < -19.5^7$ from the Sloan Digital Sky Survey data release 7 (SDSS DR7, Abazajian et al. 2009). Lee et al. (2012a) identified bars in galaxies through visual inspection of SDSS color images. They classified barred galaxies into three types based on the relative size of bars (i.e. strong, weak and ambiguous), which agrees well with the classification result of Nair & Abraham (2010). Lee et al. (2012a) also provide a sample of galaxies without bars.

The catalog contains both early- and late-type galaxies with an axis ratio $b/a > 0.6$ where bar classification is reliable. Galaxy morphology is adopted from the Korea Institute for Advanced Study Value-Added Galaxy Catalog (KIAS VAGC; Choi et al. 2010). We use only the

sample of 10,674 late-type galaxies with strong, weak and no bars in this study: 2542 strongly-barred (23.8%), 698 weakly-barred (6.5%) and 7434 non-barred (69.7%) galaxies.

Because we are interested in star formation activity of barred galaxies, we removed galaxies with active galactic nuclei (AGNs). These include optical AGNs identified with the criteria of Kewley et al. (2006) based on Baldwin-Phillips-Terlevich (BPT) emission-line ratio diagrams. We also identified AGNs using the *Wide-field Infrared Survey Explorer* (WISE, Wright et al. 2010) mid-infrared color-color selection criteria of Jarrett et al. (2011) plus Mateos et al. (2012), and removed them from the sample.

We finally have a sample of 1686 strongly and 547 weakly barred galaxies at $0.02 \leq z \leq 0.05489$ and $M_r < -19.5$. To compare the physical properties of these barred galaxies with those of non-barred galaxies, we construct the control sample of barred galaxies using the non-barred galaxies. To have an unbiased control sample, we match the stellar mass and redshift distributions of barred and non-barred galaxies; we randomly select galaxies from the sample of non-barred galaxies to have the same distributions of stellar mass and redshift as for the sample of barred galaxies. We construct the control samples for strongly and weakly barred galaxies separately. Figure 1 shows stellar masses of strongly (left panels) and weakly (right panels) barred galaxies as a function of redshift with their control samples. We examine the redshift and stellar mass distributions of barred and non-barred galaxies using the Kolmogorov-Smirnov (K-S) test and the Anderson-Darling (A-D) k-sample test. Both tests cannot reject the null hypothesis that the distributions of barred and non-barred galaxies are extracted from the same parent population. We also examine the distributions of axial ratio and apparent isophotal size of barred and non-barred galaxies that can affect the measurement of star formation activity, and again find no systematic difference between the two samples.

2.2. Physical Parameters of Galaxies

The physical parameters of galaxies that we consider in this study are star formation rate (SFR), stellar mass, UV/mid-infrared photometric data, atomic and molecular gas masses, and gas metallicity. Here we briefly describe these parameters.

The SFRs of galaxies are adopted from the MPA/JHU DR7 VAGC (Brinchmann et al. 2004), which provides extinction and aperture corrected SFR estimates for SDSS galaxies. When the SFRs of galaxies cannot be directly measured from the emission lines (e.g., AGN and composite galaxies), they use the 4000 Å break (D4000) to measure SFRs (see Brinchmann et al. 2004 and the web site⁸ for details). The stellar mass estimates are also from the MPA/JHU DR7 VAGC, which are based on the fit of SDSS five-band photometry with the model of Bruzual & Charlot (2003) (see also Kauffmann et al. 2003). We convert SFR and stellar mass estimates in the MPA/JHU DR7 VAGC that are based on Kroupa initial mass function (IMF, Kroupa 2001) to those with

⁷ The r -band absolute magnitude, M_r , is based on $H_0 = 100 \text{ km s}^{-1} \text{ Mpc}^{-1}$ in Lee et al. (2012a).

⁸ <http://www.mpa-garching.mpg.de/SDSS/DR7/sfrs.html>

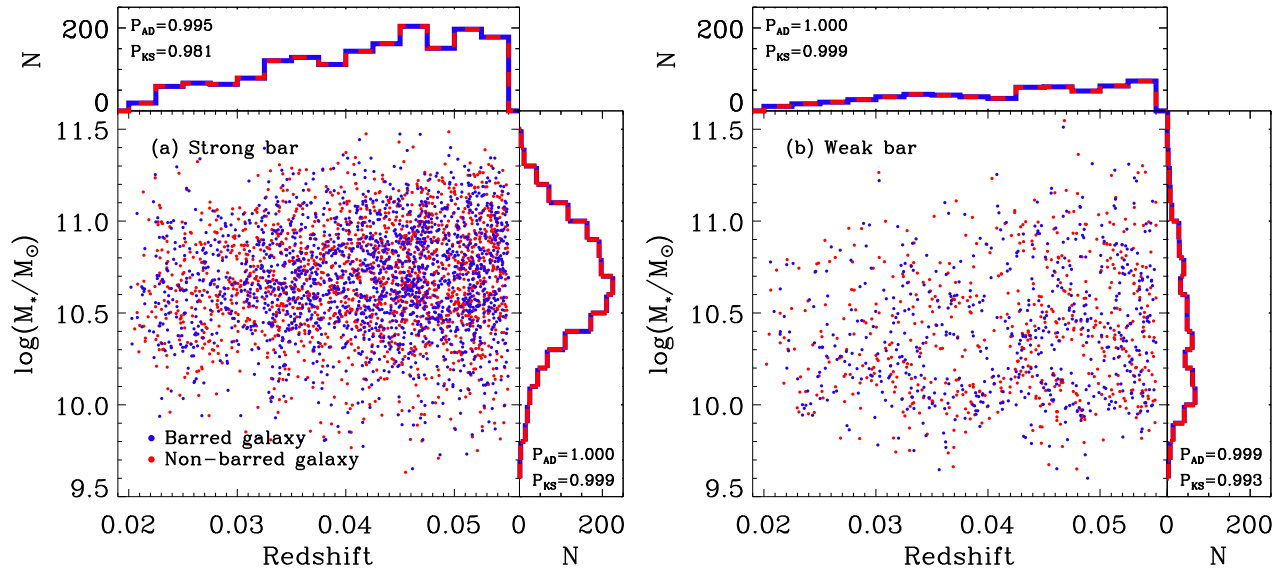


Figure 1. Stellar mass as a function of redshift for the galaxies with strong (left) and weak (right) bars. Blue and red dots represent barred and non-barred galaxies, respectively. The red histograms are the redshift and stellar mass distributions for barred galaxies, which overlap with those distributions of non-barred galaxies (blue histogram). Two numbers in each panel indicate p -values from the K-S and A-D k-sample tests on the distributions of barred and non-barred galaxies.

Salpeter IMF (Salpeter 1955) by dividing them by a factor of 0.7 (Elbaz et al. 2007). The gas metallicity (i.e. gas-phase oxygen abundance) is also adopted from the MPA/JHU DR7 VAGC (Tremonti et al. 2004).

We used the multiwavelength photometric data of SDSS galaxies compiled in Hwang & Geller (2013). The near-UV data are taken from the *Galaxy Evolution Explorer* (GALEX, Martin et al. 2005) general release 6 (GR6), which provides a cross-matched table (xSDSSDR7) against the SDSS DR7. We also include the mid-infrared data from the *WISE* all-sky survey catalog (Wright et al. 2010). The catalog provides uniform photometric data for over 747 million objects at four mid-infrared bands (3.4, 4.6, 12, and 22 μm). The matching tolerance between the SDSS and *WISE* objects is $3''$. We adopt the point source profile-fitting magnitudes, and use only the flux density with the signal-to-noise ratio $S/N \geq 3$ at each band.

The atomic gas mass, M_{HI} , is adopted from the 70 per cent data ($\alpha.70$) of the Arecibo Legacy Fast ALFA Survey (ALFALFA, Giovanelli et al. 2005; Haynes et al. 2011), which provides HI data for 25,535 galaxies at $z < 0.06$. The molecular gas mass, M_{H_2} , is collected from the CO Legacy Database for GASS (COLDGASS, Saintonge et al. 2011) and the Atacama Pathfinder Experiment (APEX) Low-redshift Legacy Survey for MOlecular Gas (ALLSMOG, Bothwell et al. 2014). Among the 1686 strongly barred galaxies (their control sample has the same number of galaxies), there are 318 barred and 397 non-barred galaxies with HI detections, and are 11 barred and 23 non-barred galaxies with H_2 detections. Among the 547 weakly barred galaxies, there are 149 barred and 135 non-barred galaxies with HI detections, and are 3 barred and 9 non-barred galaxies with H_2 detections.

3. RESULTS

3.1. Star Formation Activity of Barred Galaxies

The top panels of Figure 2 show the SFRs of barred (blue dots) and non-barred (red dots) galaxies as a function of stellar mass. The left and right panels display strongly and weakly barred galaxies, respectively. We also show the locus of main-sequence star-forming galaxies defined in Elbaz et al. (2007). The solid line is the best-fit to the SDSS main sequence star-forming galaxies, and the upper and lower dashed lines are a factor 4 above and below this fit. We adopt the main-sequence locus of Elbaz et al. (2007) for ease of comparison with other studies, and note that the following results do not change much even though we newly define the main sequence using the galaxies in this study.

We then consider the galaxies within these dashed lines as main sequence (MS), those above the upper dashed line as starburst (SB, $\text{SFR} > 4 \times \text{SFR}_{\text{MS}}$), and those below the lower dashed line as quiescent galaxies (QS, i.e. $\text{SFR} < 0.25 \times \text{SFR}_{\text{MS}}$). The majority of our samples of barred and non-barred galaxies are in the main sequence as expected. It is difficult to tell the difference in the distributions of barred and non-barred galaxies in this SFR- M_* plane by eye, consistent with previous results (Willett et al. 2015). Weakly barred galaxies tend to have more low-mass galaxies with $M_* < 3 \times 10^{10} M_\odot$ than high-mass galaxies, which is different from the case of strongly barred galaxies. The bottom panels show the specific SFRs (sSFRs) for the same samples as a function of stellar mass. Both strongly and weakly barred galaxies follow the tight star-forming sequence.

We calculate the fraction of galaxies in each group of star-formation mode, and summarize the result in Table 1. The fraction of main-sequence galaxies is very high for both strongly and weakly barred galaxies as expected, but is lower in strongly barred galaxies than in weakly barred galaxies. The left columns for strongly barred galaxies show that the fractions of starburst and main sequence galaxies are smaller in barred galaxies than in non-barred galaxies; the fraction of quiescent galaxies for strongly barred galaxies is larger than for non-barred

Table 1
Number and Fraction of Galaxies in Each Group

Type	Strongly Barred Galaxies		Weakly Barred Galaxies	
	Bars	No Bars	Bars	No Bars
Starburst	3 (0.2±0.1%)	11 (0.7±0.1%)	4 (0.7±0.1%)	10 (1.8±0.1%)
Main Sequence	1065 (63.1±0.9%)	1139 (67.5±0.9%)	441 (80.6±1.5%)	430 (78.6±1.5%)
Quiescent	618 (36.7±0.7%)	536 (31.8±0.7%)	102 (14.7±0.7%)	107 (19.6±0.8%)
Total	1686	1686	547	547

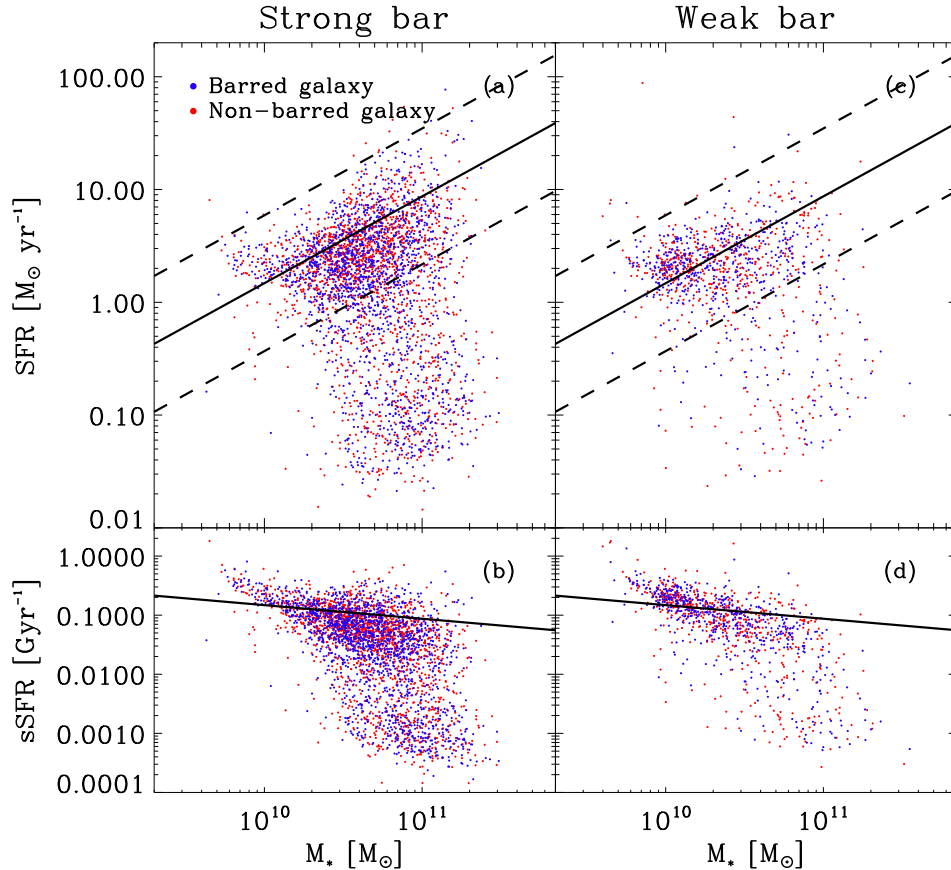


Figure 2. SFRs (left top) and sSFRs (left bottom) of galaxies as a function of stellar mass for strongly barred galaxies. Blue and red dots represent barred and non-barred galaxies, respectively. Solid lines in top and bottom panels are the best fits of the main sequence star-forming galaxies in SDSS (Elbaz et al. 2007), and the upper and lower dashed lines are a factor 4 above and below this fit. (Right) Same as left panels, but for weakly barred galaxies and their control sample.

galaxies accordingly. The error represents 68% (1σ) confidence interval that is determined by the bootstrap resampling method. Considering the errors, the difference between strongly barred galaxies and their control sample is not negligible. However, the fraction of each group for weakly barred galaxies is similar to that for their control sample.

To better compare the star formation activity between barred and non-barred galaxies by minimizing the mass effects, we plot the starburstiness (R_{SB}) distribution in Figure 3. The starburstiness is a measure of the excess in sSFR of a galaxy compared to sSFR of a main-sequence star-forming galaxy with the same mass, and is defined by $R_{SB} = sSFR/sSFR_{MS}$ (Elbaz et al. 2011). Figure 3 displays the starburstiness distributions of strongly (left panel) and weakly (right panel) barred galaxies. The left panel shows that the strongly barred galaxies (blue histogram) have a wider, lower peak than their control

sample (red histogram) at $R_{SB} \approx 0.7$. The K-S and A-D k-sample tests on the starburstiness distributions of strongly barred galaxies and their control sample yield p -values of $p_{KS} < 0.001$ and $p_{AD} < 0.006$, indicating a significant difference between the two distributions. However, the right panel for weakly barred galaxies shows no such difference between barred (blue histogram) and non-barred (red histogram) galaxies, confirmed by the K-S and A-D k-sample tests.

To explore a possible mass dependence of the starburstiness distribution, we also examine the starburstiness distributions at several narrow mass ranges (not shown here, but from $\log(M_*/M_\odot) = 9.5$ to $\log(M_*/M_\odot) = 11$ with a 0.5 dex bin). The histogram at each mass bin shows the similar results to the one using all the galaxies (i.e. statistically different distribution between strongly-barred galaxies and their control sample except the mass range of $10.0 < \log(M_*/M_\odot) < 10.5$, and

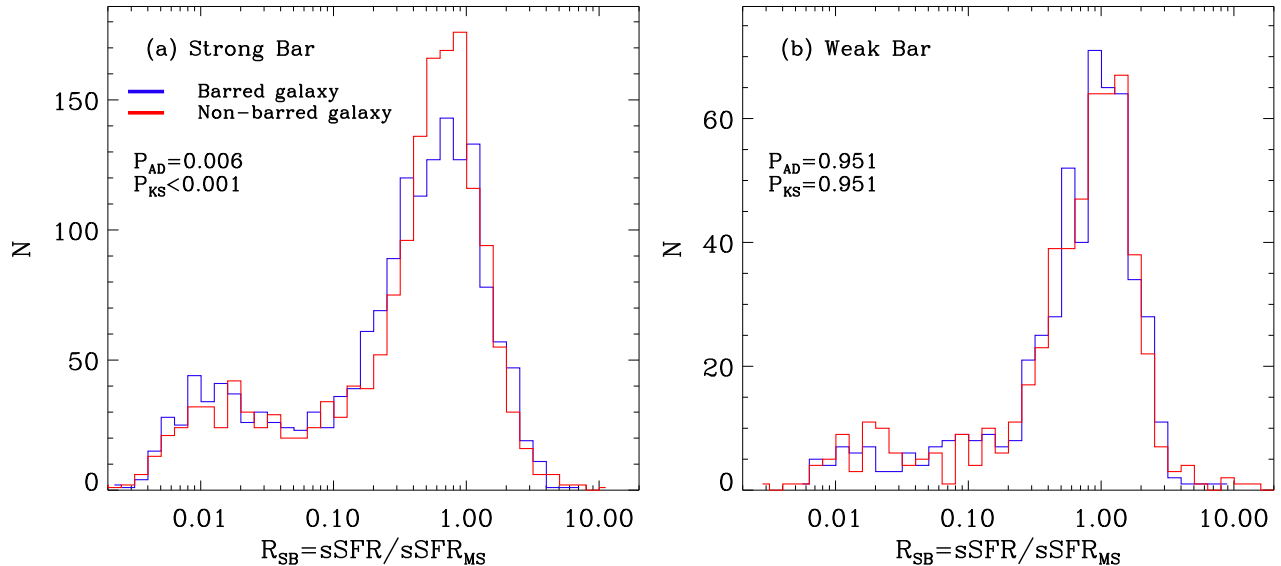


Figure 3. Starburstiness R_{SB} distributions of strongly (left) and weakly (right) barred galaxies and their control samples. Blue and red lines represent barred and non-barred galaxies, respectively.

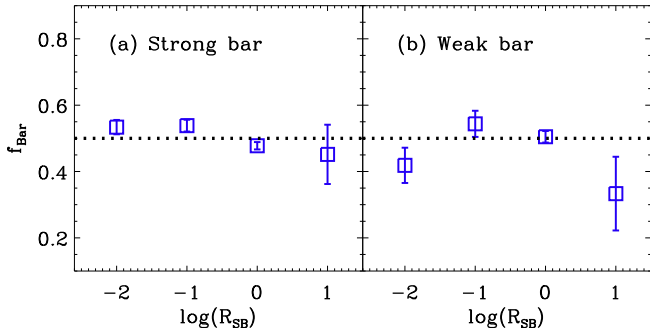


Figure 4. Barred galaxy fraction as a function of starburstiness, $\log(R_{SB})$: (left) strongly barred galaxies, (right) weakly barred galaxies. The dashed line represents $f_{\text{Bar}} = 0.5$.

no statistically difference between weakly-barred galaxies and their control sample), suggesting that the starburstiness difference between barred and non-barred galaxies persists throughout the entire mass range.

When we compare R_{SB} distributions between strongly and weakly barred galaxies, the strongly barred galaxies appear to have a relatively higher fraction of quiescent galaxies ($R_{SB} \approx 0.01$) than the weakly barred galaxies (see also Table 1). The K-S and A-D k-sample tests on the starburstiness distributions of strongly and weakly barred galaxies reject the null hypothesis at $>3\sigma$ level, suggesting a significant difference in the star formation activity between the two.

To better understand the correlation between the presence of bars and the starburstiness of galaxies, we show the fraction of barred galaxies as a function of starburstiness in Figure 4. The left panel for the strongly barred galaxies shows a hint of decrease of bar fraction with starburstiness, but it is not conclusive because of large error bars. The weakly barred galaxies in the right panel show no clear dependence of bar fraction on the starburstiness.

3.2. Comparison of Physical Parameters between Barred and Non-barred Galaxies

3.2.1. Multiwavelength Data from near-UV to mid-infrared

Figure 5 shows several multiwavelength colors of barred and non-barred galaxies as a function of stellar mass (left: strongly barred galaxies, right: weakly barred galaxies). Beginning from the top panel, we display, sequentially, $g-r$, $\text{NUV}-r$, mid-infrared $[3.4]-[12]$ colors, the flux ratios between $\text{H}\alpha$ and $\text{H}\beta$ (i.e., Balmer decrement), and D_n4000 . The optical $g-r$ color is a good tracer of star formation activity in galaxies (e.g., Strateva et al. 2001; Blanton et al. 2003). The $\text{NUV}-r$ and $[3.4]-[12]$ colors are good indicators of recent star formation activity of galaxies with slightly different timescales (e.g., Ko et al. 2013, 2016; Lee et al. 2015, 2017); both NUV and mid-infrared are sensitive to very recent (< 1 Gyr) star formation, but only the mid-infrared is sensitive to star formation over longer (up to ~ 2 Gyr) timescales. The flux ratio between $\text{H}\alpha$ and $\text{H}\beta$ (i.e., Balmer decrement) is a measure of dust extinction. When there is no dust in galaxies, $\text{H}\alpha/\text{H}\beta$ ratios are expected to be 2.86 and 3.1 for star-forming and AGN-host galaxies, respectively (in the nominal case B recombination for $T = 10,000$ K and $n_e \approx 10 \text{ cm}^{-3}$, Osterbrock & Ferland 2006). Therefore, flux ratios larger than these values indicate dust extinction. D_n4000 is a measure of the 4000 \AA break (Bruzual 1983; Balogh et al. 1999), which results from an accumulation of absorption lines of ionized metals in low mass stars at wavelength $< 4000 \text{ \AA}$. The amplitude of the break is smaller in galaxies with young stellar populations because the opacity decreases in hot young stars. It is larger for old metal-rich populations. Therefore, D_n4000 is a useful measure of the age of the stellar population.

Figure 5 shows that as stellar mass increases, $g-r$ and $\text{NUV}-r$ colors increase (Blanton et al. 2003; Lee et al. 2012b; Ko et al. 2013), $[3.4]-[12]$ color decreases (Ko et al. 2013), and D_n4000 increases (Geller et al. 2014, 2016). The difference between barred and non-barred galaxies in each mass bin is not obvious. To minimize the mass effects on the comparisons of color distributions between the two samples, we show the histogram of each parameter for the galaxies in a narrow

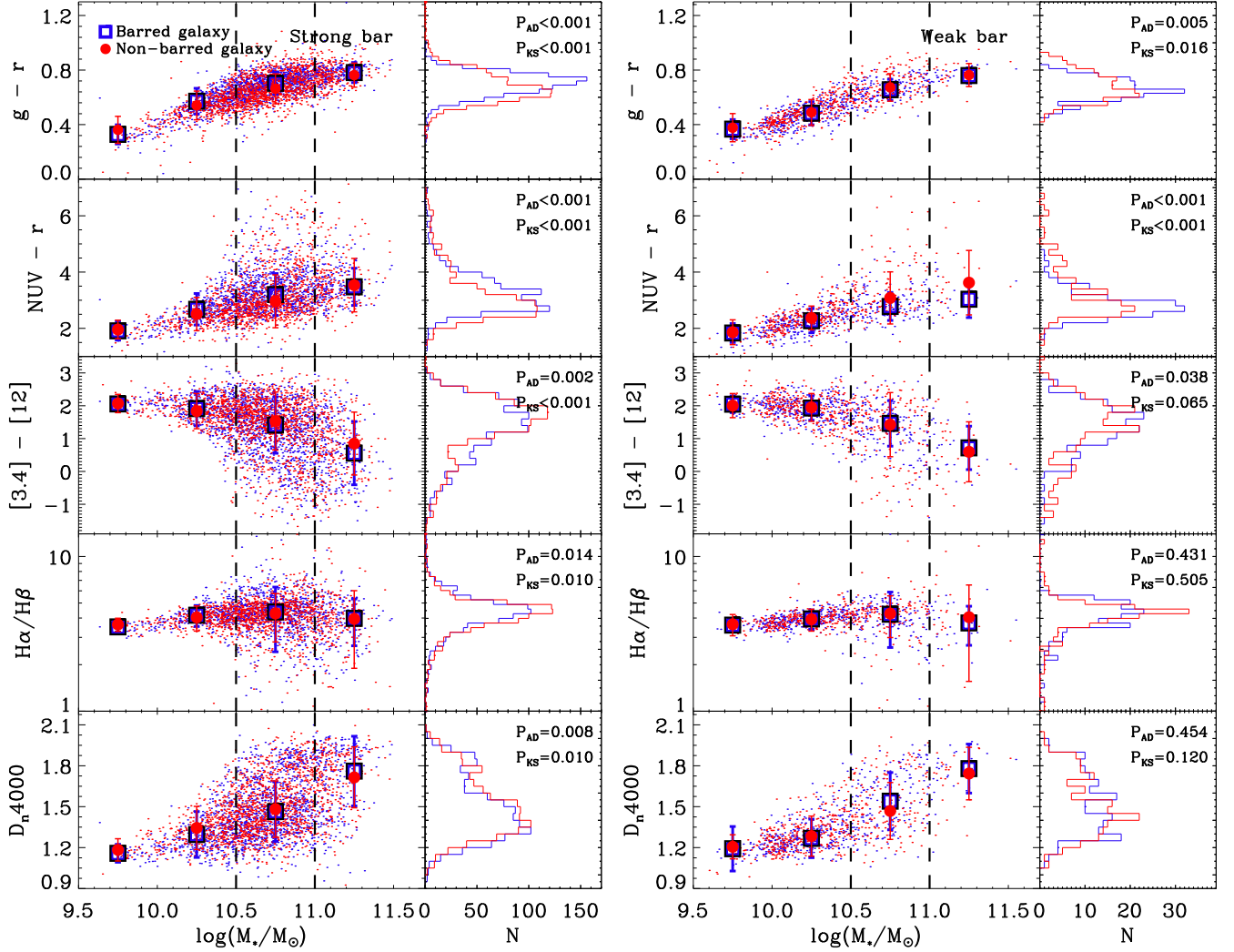


Figure 5. (Left) Optical, near-UV, mid-IR colors, Balmer decrement (H_{α}/H_{β}) and D_n4000 (from top to bottom) as a function of stellar mass for strongly barred galaxies (blue dots) and their control sample (red dots). Large blue open square and red filled circle are median values for barred and non-barred galaxies at each mass bin, respectively. The histogram in each panel shows the distribution of each parameter for barred (blue line) and non-barred (red line) galaxies in a narrow mass range $10.5 \leq \log(M_*/M_{\odot}) < 11.0$. (Right) Same as left panels, but for weakly barred galaxies and their control sample.

mass bin (i.e. $10.5 \leq \log(M_*/M_{\odot}) < 11.0$), as indicated with vertical dashed lines in Figure 5 where we can have a large number of galaxies. The strongly barred galaxies tend to be redder in $g-r$ and $NUV-r$ colors, and bluer in $[3.4]-[12]$ color than their control sample. This systematic difference in colors between the strongly barred galaxies and their control sample seems to result from the different dust extinction between the two. The second panel from the bottom shows that there is a statistically significant difference in the Balmer decrement distribution between strongly-barred galaxies and their control sample; barred galaxies appear to experience slightly more dust extinction than non-barred galaxies, which can make the barred galaxies redder in $g-r$ and $NUV-r$ colors. There also could be an additional effect on this color difference, which is hinted by the smaller number of actively star-forming galaxies in the sample of strongly barred galaxies than in their control sample in Figure 3.

On the other hand, D_n4000 does not show a systematic difference between strongly barred galaxies and their control sample. Although the K-S and A-D k-sample tests on D_n4000 distribution at $10.5 \leq \log(M_*/M_{\odot}) < 11.0$ indicate a significant difference between the two, the Student's t-test suggests that the probability that the two samples have significantly different means is only at $< 2\sigma$ level; this means that the low p -values of the K-S and A-D k-sample tests are not because of different means (or medians) but because of different distributions. The right panels for the weakly barred galaxies show that barred and non-barred galaxies are statistically different only in the $NUV-r$ color distribution.

3.2.2. Gas Properties

Star formation activity is directly connected to the amount of gas in galaxies. We therefore compare the amounts of atomic (HI) and molecular (H_2) gas between barred and non-barred galaxies. Figure 6 shows the frac-

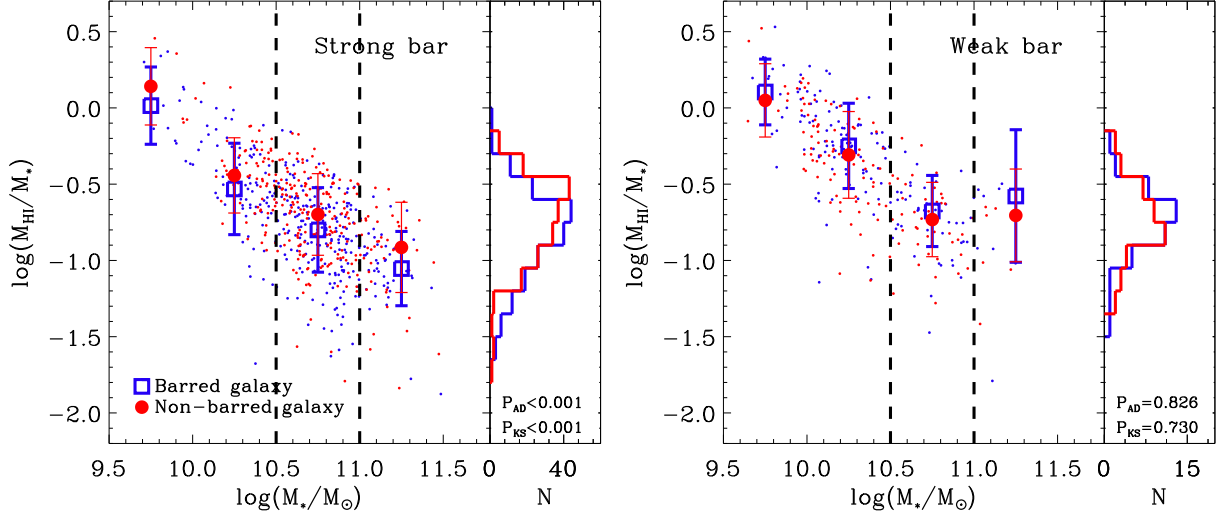


Figure 6. (Left) Mass fraction of HI gas as a function of stellar mass for strongly barred galaxies and their control sample. Blue and red dots show barred and non-barred galaxies, respectively. Blue open rectangles and red filled circles are median values at different mass bins. The right panel shows the histograms of gas fraction for barred (blue line) and non-barred (red line) galaxies. (Right) Same as left panels, but for weakly barred galaxies and their control sample.

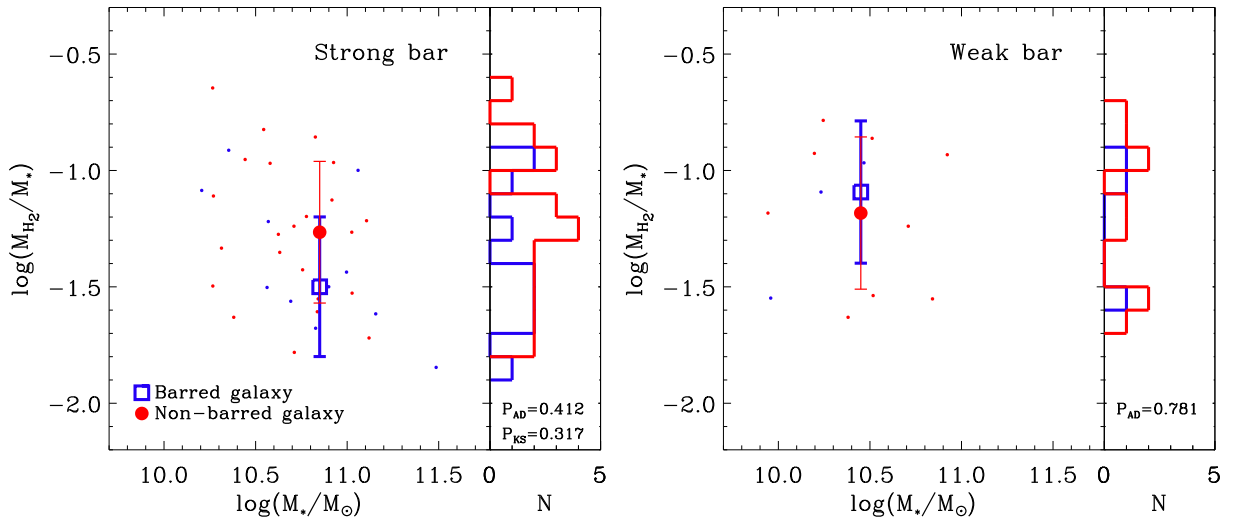


Figure 7. Same as Figure 6, but for H₂ gas mass fraction.

tion of HI gas mass as a function of stellar mass for our samples. As expected, the HI gas fraction decreases with stellar mass. The left panel for strongly barred galaxies shows that the HI gas fraction of barred galaxies is systematically lower than that of non-barred galaxies, consistent with the results in previous studies (Masters et al. 2012; Cervantes Sodi 2017). The K-S and A-D k-sample tests on the HI gas fraction distributions between the two also reject the null hypothesis that the two distributions are extracted from the same parent population at $>3\sigma$ level. Interestingly, the weakly barred galaxies in the right panel appear to have higher HI gas fractions than non-barred galaxies in all mass bins, different from the case of strongly barred galaxies. However, the difference is not statistically significant.

We also show the fraction of H₂ gas mass as a function of stellar mass in Figure 7. The left panel for strongly barred galaxies shows a hint of different H₂ gas fractions

between barred and non-barred galaxies (i.e. lower gas fraction in barred galaxies), similar to the result of HI gas fraction. However, the difference is not statistically significant as the K-S and A-D tests suggest. The right panel for the weakly barred galaxies does not show any meaningful comparison between barred and non-barred galaxies because of small number statistics.

We also examine the distribution of gas depletion time, $t_{\text{dep}} \equiv M_{\text{gas}}/\text{SFR}$ for both HI and H₂ gas, but do not find any significant difference between barred and non-barred galaxies for both strongly and weakly barred galaxies (not shown here).

Figure 8 shows a comparison of gas metallicity between barred and non-barred galaxies. The metallicity of galaxies increases with stellar mass, which follows a well-known mass-metallicity relation (Lequeux et al. 1979; Tremonti et al. 2004; Zahid et al. 2013). The metallicity of strongly barred galaxies is systematically higher than

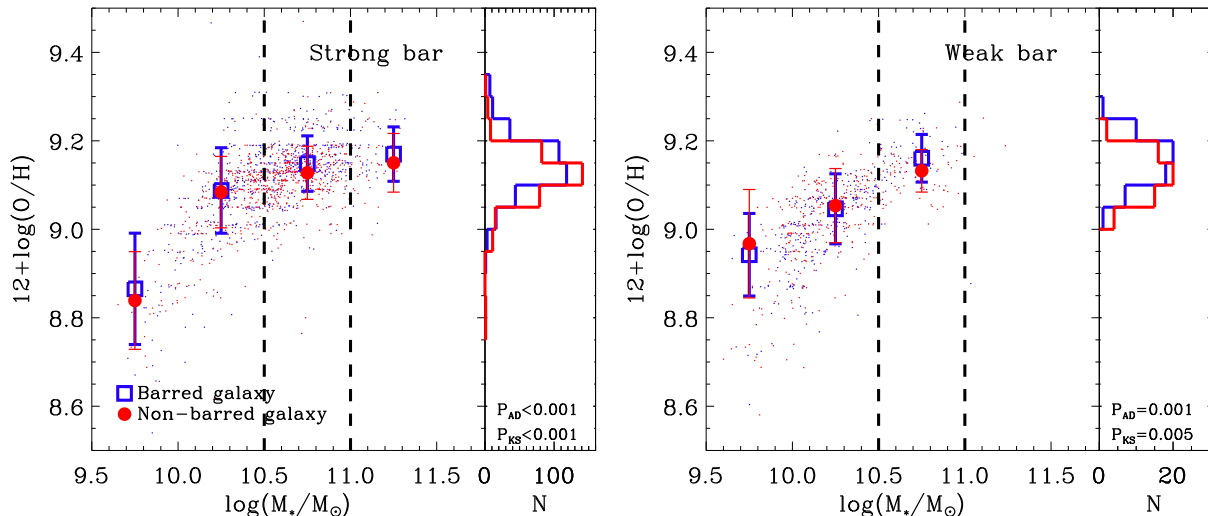


Figure 8. Same as Figure 6, but for gas metallicity.

of their control sample at each mass bin. This is confirmed by the K-S and A-D k-sample tests at $> 3\sigma$ level, consistent with the results of Vera et al. (2016). Overall gas metallicity between weakly-barred galaxies and their control sample is similar (confirmed by the K-S and A-D k-sample tests), but the galaxies at $10.5 \leq \log(M_*/M_\odot) < 11.0$ show a $> 2.8\sigma$ difference.

3.3. Stellar Populations of Barred Galaxies: Fit to the Optical Spectra with STARLIGHT

In this section, we compare stellar populations of barred and non-barred galaxies. We perform a decomposition of stellar populations of barred and non-barred galaxies by fitting the SDSS optical spectra with the spectral fitting code, STARLIGHT (Cid Fernandes et al. 2005). To minimize the mass effects on the stellar population comparison and to increase the signal-to-noise ratio of the spectra, we divide the galaxy samples into four mass bins and stack the rest-frame spectra in each mass bin. We normalize the individual spectrum at rest-frame 4150–4250 Å and take the median for the stacking. The wavelength coverage for the stacked spectra is 3800 – 7650 Å. We fit to the spectra using 45 spectral templates of Bruzual & Charlot (2003) with 15 ages (between 1 Myr and 13 Gyr) and 3 metallicities ($Z = 0.004, 0.02, 0.05$). These templates are generated from STELIB library (Le Borgne et al. 2003) with Padova evolutionary tracks Bertelli et al. (1994) and Chabrier (2003) IMF. We perform the STARLIGHT fit 100 times with different seeds for the random number generator and adopt the medians of derived parameters as the best-fit results. Figure 9 shows the stacked spectra of galaxies in different mass bins (gray lines) with the best-fit STARLIGHT models for barred (blue lines) and non-barred (red lines) galaxies.

The top panels of Figure 10 show the resulting mass fractions of different stellar populations for strongly barred galaxies and their control sample. As expected, the mass fractions of young (≤ 2 Gyr) and intermediate-age (~ 2 –5 Gyr) populations decrease with stellar mass for both barred and non-barred galaxies. The difference in the mass fraction between barred and non-barred

galaxies is not obvious. The weakly barred galaxies in the bottom panels show similar trends; the mass fraction of old stellar populations increases with stellar mass, and the difference between barred and non-barred galaxies is not significant.

To make a more quantitative comparison between barred and non-barred galaxies, we plot the mass fraction of young stellar population with age < 2 Gyrs in Figure 11. Both barred and non-barred galaxies show that the mass fraction of young stellar population decreases with stellar mass, which confirms the visual impression of Figure 10. At the lowest mass bin ($9.5 < \log(M_*/M_\odot) < 10.0$), the strongly barred galaxies show a possible hint of lower mass fraction of young stellar population than in non-barred galaxies, but it is not statistically significant. The weakly barred galaxies in the right panel show a pattern different from strongly barred galaxies (i.e. higher mass fraction of young stellar population in barred galaxies than in non-barred galaxies), but again it is not statistically significant. Ko et al. (2016) examined the dependence of the fit on the choice of spectral templates with various combinations of age/metallicity distributions (i.e. different star formation history), stellar population models, and IMFs. They found that the mass fraction of young and intermediate-age stars does not change much with different combinations of age and metallicity distributions, which suggests that our results would not change much with different choices of spectral templates for the fit.

4. DISCUSSION

We use various tracers of star formation activity in galaxies to examine the difference between barred and non-barred galaxies. The comparisons of starburstiness, $g-r$, $NUV-r$, mid-infrared [3.4]–[12] colors, the HI gas fraction, and gas metallicity between strongly barred galaxies and their control sample show significant differences between the two; the barred galaxies generally show weaker star formation activity than non-barred galaxies. The H_2 gas fraction and the mass fraction of young stellar population (< 2 Gyrs) from the decomposition of the optical spectra also show similar differences,

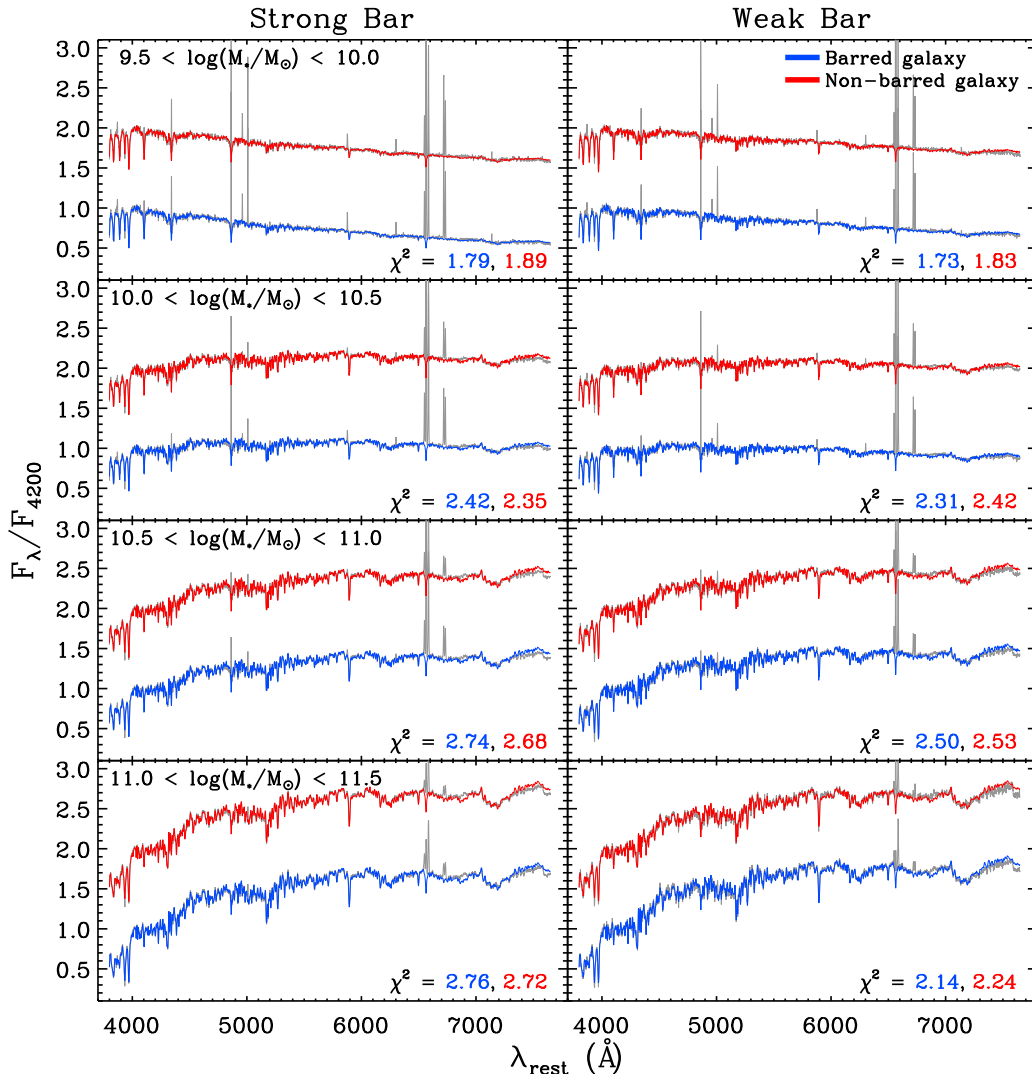


Figure 9. (Left) STARLIGHT fit to the stacked spectra of strongly barred galaxies and their control sample at different stellar mass bins. We shift the spectra of non-barred galaxies by adding unity for clarity. The gray and color-coded lines represent the stacked spectra and the best-fit models, respectively. Lines are not clearly visible because of overlap. (Right) Same as for left panels, but for weakly barred galaxies and their control sample.

but the statistical significance is not very high. On the other hand, most star formation activity tracers for the weakly barred galaxies show no such differences between barred and non-barred galaxies.

The weaker star formation activity of strongly barred galaxies than their control sample is consistent with previous results (Vera et al. 2016). Because the weakly barred galaxies show no such difference, comparisons between barred and non-barred galaxies including both strongly and weakly barred galaxies would have made the possible difference weak, which can result in no increase in star formation activity in barred galaxies (Pompea & Rieke 1990; Martinet & Friedli 1997; Chapelon et al. 1999; Cheung et al. 2013; Willett et al. 2015).

We also show that the HI gas fraction of strongly barred galaxies is, on average, lower than their control sample, confirming the previous findings (Cervantes Sodi 2017) even though some studies did not distinguish strongly and weakly barred galaxies (Masters et al. 2012). Figure 7 shows a hint of lower

H₂ gas fraction in barred galaxies than in non-barred galaxies, but it needs to be examined with more H₂ gas mass measurements of galaxies for better statistical significance. We could not find a significant difference in the distribution of gas depletion time between barred and non-barred galaxies for both HI and H₂ gas. Similarly, Saintonge et al. (2012) found only a marginal difference in molecular gas depletion time between barred and non-barred galaxies. Cervantes Sodi (2017) also found that only strongly barred galaxies show a mild increase of bar fraction with atomic gas depletion time.

Many numerical simulations showed that the star formation activity in central regions of galaxies could be enhanced by the presence of galactic bars (Shlosman et al. 1990; Athanassoula 1994; Combes 2001; Kim et al. 2011). Although at first instance our results seem at odds with these theoretical expectations, we explore two scenarios that can help to ease the discrepancy. First, Carles et al. (2016) suggested that the star formation activity of barred galaxies could be triggered when the bars are formed and the SFRs of barred galaxies be-

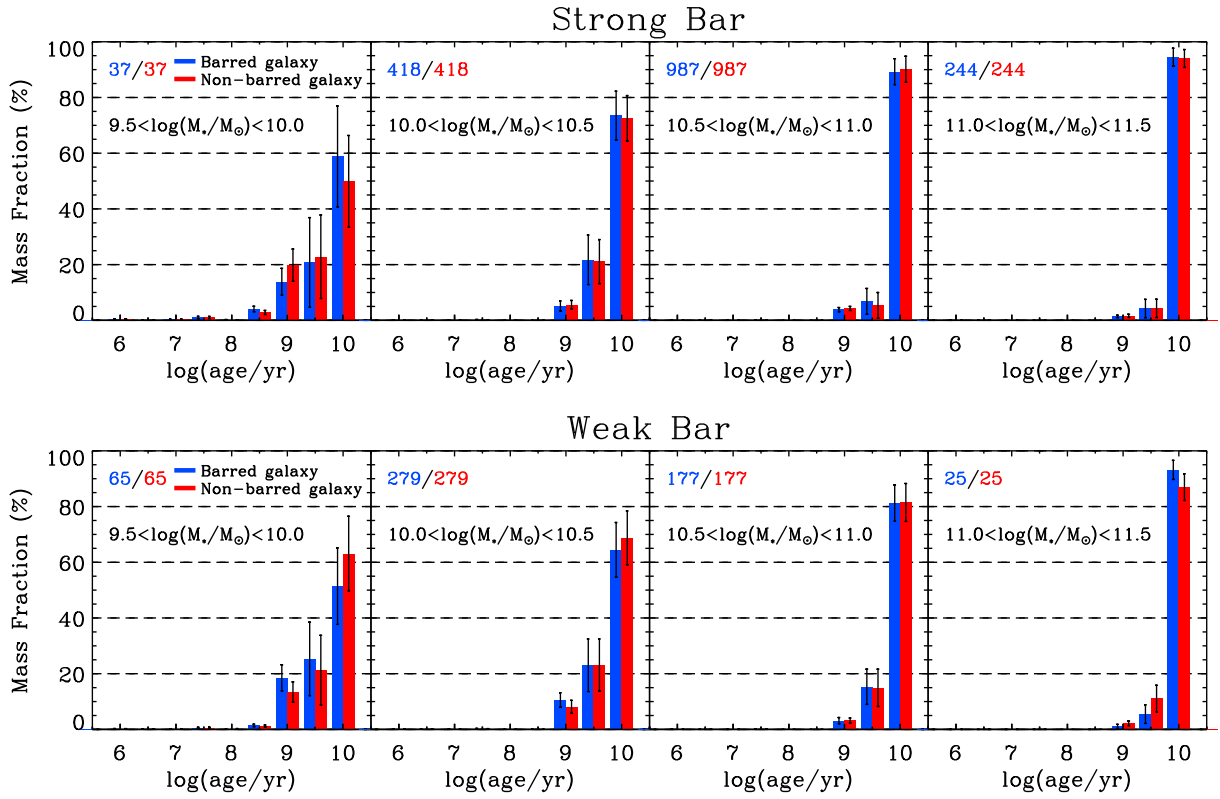


Figure 10. (Top) The fractions of stellar populations with different ages in the total stellar mass for strongly barred galaxies (blue histograms) and their control sample (red histograms) at different mass bins. Error bars indicate 1σ distributions from the 100 fits with different seeds. (Bottom) Same as top panels, but for weakly barred galaxies and their control sample.

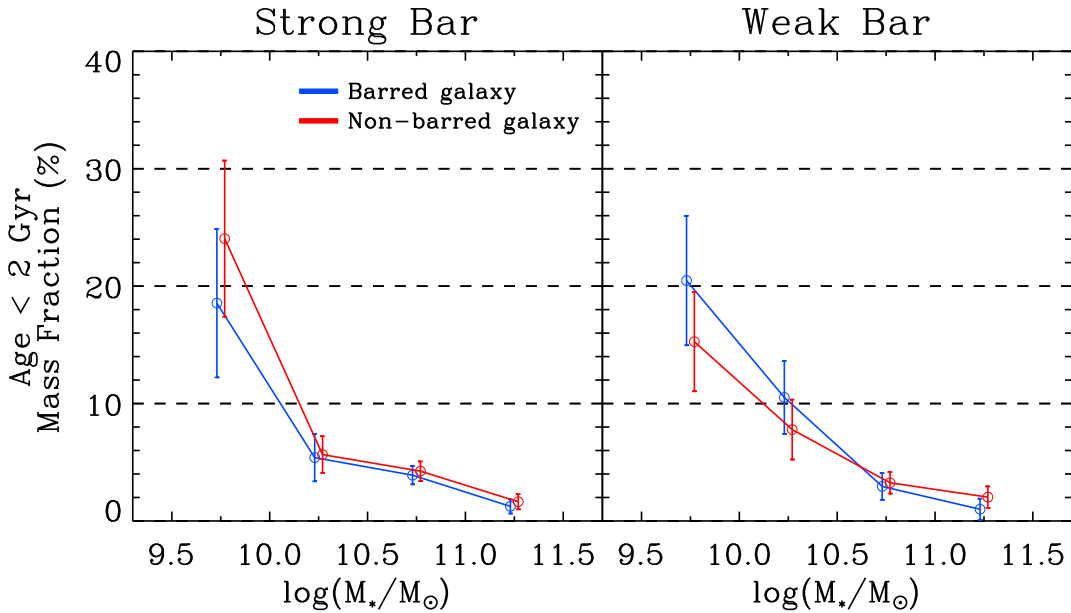


Figure 11. (Left) The mass fractions of young stellar populations (< 2 Gyr) as a function of stellar mass for strongly barred galaxies (blue circles) and their control sample (red circles). (Right) Same as left panels, but for weakly barred galaxies and their control sample.

come similar to or lower than non-barred galaxies in 2 Gyrs; the difference between barred and non-barred galaxies would be larger strongly barred galaxies. The consumption of hydrogen gas is accelerated along with the star formation activity in barred galaxies, then the amount of gas in barred galaxies also becomes similar to or lower than for non-barred galaxies. These could explain why many observations show no increase in *current* star formation activity of barred galaxies compared to non-barred galaxies. These also could explain lower gas mass and higher metallicity currently in barred galaxies than in non-barred galaxies. This was the motivation of the decomposition of the stellar populations of barred and non-barred galaxies by fitting to the SDSS spectra with STARLIGHT in this study. However, our decomposition could not find any significant difference in the mass fraction of young stellar populations (< 2 Gyrs) between barred and non-barred galaxies even though there is a hint of difference only at the lowest mass bin ($9.5 < \log(M_*/M_\odot) < 10.0$).

Second, the star formation indicators we consider in this study are global galaxy parameters rather than central ones, and the bar-induced star formation activity is expected to take place only in central regions where bars can shock the gas. Observational evidence of this localized star formation in the central region of barred galaxies has already been reported. For instance, by studying the central-to-total star formation activity in a large volume-limited sample of SDSS galaxies, Wang et al. (2012) found that more than half of the galaxies with enhanced central star formation activity have bars. More recently, Lin et al. (2017) analyzed the integral field spectroscopic data of 57 galaxies, and found that among the 17 “turnover” galaxies with rejuvenated pseudobulges most of them (15/17) have bars. More two-dimensional spectroscopic observations of these barred galaxies will be useful for better localizing the star formation activity in barred galaxies.

If bar-triggered star formation is not reflected globally, it would be difficult to imagine these systems being efficient in exhausting their gas though enhanced star formation. In this case, the low gas fraction in barred galaxies could be explained through the inhibiting effect that the gas has in the formation and growth of bars (i.e. bars form later and grow more slowly in gas-rich galaxies than in gas-poor galaxies), as shown in hydrodynamical simulations (Villa-Vargas et al. 2010; Athanassoula et al. 2013). We could not distinguish which scenario is more plausible at this stage, but studying barred galaxies at high redshift to understand their evolution will be helpful for testing these scenarios.

Bar strength has been considered as one of important parameters in the star formation activity of barred galaxies (Athanassoula 2003; Buta et al. 2005; Nair & Abraham 2010; Hoyle et al. 2011). In this study, we construct the control samples of non-barred galaxies for strongly and weakly barred galaxies separately by matching the stellar mass and redshift distributions. Our results suggest that many physical properties of strongly and weakly barred galaxies could be different; the current star formation activity of strongly barred galaxies appears lower than that of their control sample, but the weakly barred galaxies do not differ much from their control sample. If we assume that weak bars in galaxies

evolve into strong bars and that the star formation activity is enhanced because of the presence of bars, we expect enhanced star formation activity in weakly barred galaxies compared to non-barred galaxies. However, we found no significant difference in star formation activity between weakly barred galaxies and their control sample. This can suggest that weakly and strongly barred galaxies are not linked by an evolutionary sequence or that the star formation activity of galaxies is not strongly affected by the presence of bars.

We note that the barred galaxy sample used in this study is constructed from the visual inspection of SDSS images with a typical seeing ~ 1.4 arcsec (Lee et al. 2012a). To identify bars in galaxies, the size of bars should be typically 3–4 times larger than the point spread function (PSF) size. This means that some bars smaller than 2–5 kpc at $0.02 \leq z \leq 0.05$ (i.e. redshift range in our sample) could be missed in our galaxy sample because of seeing effect. This can partly explain why some studies using nearby galaxy samples found higher bar fractions than other studies that use relatively more distant galaxy samples (e.g. Menendez-Delmeestre et al. 2007; Díaz-García et al. 2016). On the other hand, the size of bars increases with galaxy mass. Then Figure 20 in Díaz-García et al. (2016) suggests that a significant amount of barred galaxies less massive than a few times $10^{10} M_\odot$ could be missed in our galaxy sample because of the spatial resolution limit (i.e. $r_{\text{bar}} \lesssim 2$ kpc). This means that some less massive galaxies classified as non-barred galaxies in our sample could indeed be barred galaxies. This can explain why some of the differences in physical parameters between barred and non-barred galaxies are only prominent for relatively more massive galaxies (e.g. $10.5 < \log(M_*/M_\odot)$).

5. CONCLUSIONS

We use samples of strongly and weakly barred galaxies in the local universe, and compare their physical properties with those of non-barred galaxies focusing on the star formation activity. Our primary results are:

1. The distributions of starburstiness (R_{SB}), a measure of the excess in sSFR of a galaxy compared to the sSFR of a main sequence star-forming galaxy, for strongly barred galaxies and their control sample are different; the strongly barred galaxies have a wider, lower peak near main sequence and have more quiescent galaxies than their control sample. However, the starburstiness distribution of weakly barred galaxies is similar to that of their control sample.
2. The $g-r$, NUV- r , and mid-infrared [3.4]–[12] colors of strongly barred galaxies are statistically different from those of their control sample. These color differences seem to result from the different dust extinction between the two, evidenced by the Balmer decrement (H_α/H_β). There also could be an additional effect on this color difference, which is that the star formation activity of strongly barred galaxies is, on average, lower than that of non-barred galaxies. On the other hand, weakly barred galaxies do not show such significant differences in these multiwavelength parameters.

3. The HI gas fraction of strongly barred galaxies, on average, is lower than the one of their control sample. There is also a hint of different H₂ gas fraction between strongly barred galaxies and their control sample, which needs to be confirmed with more data. Gas metallicity of strongly barred galaxies is, on average, higher than for their control sample. Again, weakly barred galaxies do not show such significant differences in these gas properties.
4. The stellar population analysis of the optical spectra shows no significant difference between barred and non-barred galaxies. However, strongly barred galaxies show a possible hint of lower mass fraction of a young stellar population than in non-barred galaxies only at the lowest mass bin ($9.5 < \log(M_*/M_\odot) < 10.0$). Interestingly, weakly barred galaxies show a hint of higher mass fraction of a young stellar population than their control sample in the same mass bin.

Our results appear consistent with the idea that the star formation activity of strongly barred galaxies was enhanced in the past and is currently low (e.g. Carles et al. 2016). Because of large gas consumption along with the star formation in the past, the amount of gas and the gas metallicity of strongly barred galaxies are also expected to be currently low and high, respectively, consistent with our results. This star formation history depends on the strength of bars. To better understand the star formation activity in barred galaxies, a systematic survey of barred galaxies with two-dimensional spectroscopy and studying high-redshift barred galaxies will be helpful.

We thank the anonymous referee for helpful comments. SSK and EK were supported by the National Research Foundation grant funded by the Ministry of Science, ICT and Future Planning of Korea (NRF-2014R1A2A1A11052367). BCS acknowledges financial support through PAPIIT project IA103517 from DGAPA-UNAM. Funding for the SDSS and SDSS-II has been provided by the Alfred P. Sloan Foundation, the Participating Institutions, the National Science Foundation, the U.S. Department of Energy, the National Aeronautics and Space Administration, the Japanese Monbukagakusho, the Max Planck Society, and the Higher Education Funding Council for England. The SDSS Web Site is <http://www.sdss.org/>. The SDSS is managed by the Astrophysical Research Consortium for the Participating Institutions. The Participating Institutions are the American Museum of Natural History, Astrophysical Institute Potsdam, University of Basel, University of Cambridge, Case Western Reserve University, University of Chicago, Drexel University, Fermilab, the Institute for Advanced Study, the Japan Participation Group, Johns Hopkins University, the Joint Institute for Nuclear Astrophysics, the Kavli Institute for Particle Astrophysics and Cosmology, the Korean Scientist Group, the Chinese Academy of Sciences (LAMOST), Los Alamos National Laboratory, the Max-Planck-Institute for Astronomy (MPIA), the Max-Planck-Institute for Astrophysics (MPA), New Mexico State University, Ohio State University, University of Pittsburgh, University of Portsmouth,

Princeton University, the United States Naval Observatory, and the University of Washington. This publication makes use of data products from the *Wide-field Infrared Survey Explorer*, which is a joint project of the University of California, Los Angeles, and the Jet Propulsion Laboratory/California Institute of Technology, funded by the National Aeronautics and Space Administration.

REFERENCES

- Abazajian, K. N., Adelman-McCarthy, J. K., Agueros, M. A., et al. 2009, *ApJS*, 182, 543
- Athanassoula, E. 1992, *MNRAS*, 259, 345
- Athanassoula, E. 1994, *ApJ*, 11, 11
- Athanassoula, E. 2003, *MNRAS*, 341, 1179
- Athanassoula, E., Machado, R. E. G., & Rodionov, S. A. 2013, *MNRAS*, 429, 1949
- Balogh, M. L., Morris, S. L., Yee, H. K. C., Carlberg, R. G., & Ellingson, E. 1999, *ApJ*, 527, 54
- Bertelli, G., Bressan, A., Fagotto, F., & Nasi, E., 2009, *A&AS*, 508, 335
- Binney, G., Gerhard, O. E., Stark, A. A., Bally, J., & Uchida, K. I. 1991, *MNRAS*, 252, 210
- Blanton, M. R., Hogg, D. W., Bahcall, N. A., et al. 2003, *ApJ*, 594, 186
- Brinchmann, J., Charlot, S., White, S. D. M., Tremonti, C., Kauffmann, G., Heckman, T., & Brinkmann, J. 2004, *MNRAS*, 351, 1151
- Bothwell, M. S. et al. 2014, *MNRAS*, 445, 2599
- Boselli, A. et al. 2010, *PASP*, 122, 261
- Bruzual A., G. 1983, *ApJ*, 273, 105
- Bruzual, G., & Charlot, S. 2003, *MNRAS*, 344, 1000
- Buta, R., Vasylyev, S., Salo, H., & Laurikainen, E. 2005, *AJ*, 130, 506
- Carles, C., Martel, H., Ellison, S. L., & Kawata, D. 2016, *MNRAS*, 463, 1074
- Cervantes Sodi, B., 2017, *ApJ*, 835, 80
- Chabrier, G. 2003, *PASP*, 115, 763
- Chapelon, S., Contini, T., & Davoust, E. 1999, *A&A*, 345, 81
- Cheung, E., Athanassoula, E., Masters, K. L., et al. 2013, *ApJ*, 779, 162
- Cheung, E., Trump, J. R., Athanassoula, E., et al. 2015, *MNRAS*, 447, 506
- Choi, Y.-Y., Han, D.-H., & Kim, S. S. 2010, *ApJ*, 43, 191
- Cid Fernandes, R., Mateus, A., Sodré, L., Stasińska, G., & Gomes, J. M., 2005, *MNRAS*, 358, 363
- Cisternas, M., Gadotti, D. A., Knapen, J. H., et al. 2013, *ApJ*, 776, 50
- Combes, F., & Gerin, M. 1985, *A&A*, 150, 327
- Combes F., 2001, in *Aretxaga I., Kunth D., Mujica R., eds*, *Advanced Lectures on the starbursts-AGN*. World Scientific, Singapore, p. 223
- Conotopoulos, G., & Papayannopoulos, T., *A&A*, 92, 33
- Díaz-García, S., Salo, H., Laurikainen, E. & Herrera-Endoqui, M. 2016, *Å*, 587, 160
- Devereux, L., 1987, 323, 91
- Elbaz, D., Daddi, E., Le Borgne, D., et al. 2007, *A&A*, 468, 33
- Elbaz, D., et al. 2011, *A&A*, 533, 119
- Gao, Y., & Solomon, P. M. 2004, *AJ*, 606, 271
- Geller, M. J., Hwang, H. S., Fabricant, D. G., et al. 2014, *ApJS*, 213, 35
- Geller, M. J., Hwang, H. S., Dell’Antonio, I. P., et al. 2016, *ApJS*, 224, 11
- Giovanelli, R. et al. 2005, *AJ*, 130, 2598
- Jarrett, T. H., Cohen, M., Masci, F., et al. 2011, *ApJ*, 735, 112
- Hawarden, T. G., Mountain, C. M., Leggett, S. K., & Puxley, P. J. 1986, *MNRAS*, 221, 41
- Haynes, M. P., Giovanelli, R., Martin, A. M., et al. 2011, *AJ*, 142, 170
- Heckman, T. M. 1980, *A&A*, 88, 365
- Himmel, E., van der Hulst, J. M., Kennicutt, R. C., Keel, W. C. 1990, *A&A*, 236, 333
- Ho, L. C., Filippenko, A. V., & Sargent, W. L. W. 1997, *ApJ*, 487, 591

- Hoyle, B., Masters, K. L., Nichol, R. C., et al. 2011, MNRAS, 415, 3627
- Hwang, H. S., & Geller, M. J. 2013, ApJ, 769, 116
- Kauffmann G. et al., 2003, MNRAS 341, 33
- Kim, W.-T, Seo, W.-Y., Stone, J. M., Yoon, D., & Teuben P. J. 2012, ApJ, 747, 23
- Kim, S. S., Saitoh, T. R., Jeon, M., Figer, D. F., Merritt, D., & Wada, K. 2011, ApJ, 735, L11
- Kewley, L. J., Groves, B., Kauffmann, G., & Heckman, T 2006, MNRAS, 372, 961
- Knäpen, J. H., Beckman, J. E., Heller, C. H., Shlosman, I., & de Jong, R. S. 1995, ApJ, 454, 623
- Ko, J., Hwang, H. S., Lee, J. C., & Sohn, Y.-J. 2013, ApJ, 767, 90
- Ko, J., Chung, H., Hwang, H. S., & Lee, J. C. 2016, ApJ, 820, 132
- Kormendy, J., & Kennicutt, R. C. 2004, ARA&A, 42, 603
- Kroupa, P. 2001, MNRAS, 322, 231
- Le Borgne, J.-F., Bruzual, G., Pelló, R., et al. 2003, A&A, 402, 433
- Lee, G.-H., Park, C., Lee, M. G. & Choi, Y.-Y. 2012a, ApJ, 745, 125
- Lee, G.-H., Woo, J.-H., Lee, M. G., Hwang, H. S., Lee, J. C., Sohn, J., & Lee, J. H. 2012b, ApJ, 750, 141
- Lee, G.-H., Hwang, H. S., Lee, M. G., et al. 2015, ApJ, 800, 80
- Lee, G.-H., Hwang, H. S., Sohn, J., & Lee, M. G. 2017, ApJ, 835, 280
- Lequeux, J., Peimbert, M., Rayo, J. F., Serrano, A., & Torres-Peimbert, S. 1979, A&A, 80, 155
- Lin, L., Li, C., He, Y., Xiao, T., & Wang, E. 2017, ApJ, 838, 105L
- Mateos, S., Alonso-Herrero, A., Carrera, F. J., et al 2012, MNRAS, 426, 3271
- Martin, D. C., Fanson, J, Schiminovich, D. et al. 2005, ApJ, 619, L1
- Martinet, L., & Friedli, D. 1997, A&A, 323, 363
- Masters, K. L., Nichol R. C., Haynes, M. P., et al. 2012, MNRAS, 424, 2180
- Menendez-Delmestre, K., Schinnerer, E., Jarrett et al. 2007, ApJ, 657, 790
- Morris, M, & Serabyn, E. 1996, ARA&A, 34, 645
- Nair, P. B., & Abraham, R. G. 2010, ApJ, 714, L260
- Oh, S, Oh, K., & Yi, S. K. 2012, ApJS, 198, 4
- Osterbrock, D. E., & Ferland, G. J. 2006, Astrophysics of Gaseous Nebulae and Active Galactic Nuclei, ed. Osterbrock, D. E. & Ferland, G. J.
- Pompea, S. M., & Rieke, G. H. 1990, ApJ, 356, 416
- Regan, M. W. et al. 2006, ApJ, 652, 1112
- Saintonge, A., Kauffmann, G., Kramer, C., et al., 2011, MNRAS, 415
- Saintonge, A., Tacconi, L. J., Fabello, S., et al, 2012, ApJ, 758, 73
- Salpeter, E. E., 1955, ApJ, 121, 161S
- Seo, W.-Y., & Kim, W.-T. 2013, ApJ, 769, 100
- Shin, J. et al. 2017, ApJ, accepted (arXiv:1704.09006)
- Simkin, S. M., Su, H. J., & Schwarz, M. P. 1980, ApJ, 237, 404
- Shlosman, I., Begelman, M. C., & Frank, J. 1990, ApJ, 11, 111
- Strateva, I., Ivezić, Ž., Knapp, G. R., et al. 2001, AJ, 122, 1861
- Tremonti, C. A., Heckman, T. M., Kauffmann, G., et al. 2004, ApJ, 613, 898
- Vera, M, Alonso, S., & Coldwell, G. 2016, A&A, 595, 63
- Villa-Vargas, J., Shlosman, I., & Heller, C. 2010, ApJ, 719, 1470
- Wang, J., Kauffmann, G., Overzier, R., et al. 2012, MNRAS, 423, 3486
- Willett, K. W., Schawinski, K., Simmons, B. D., et al. 2015, MNRAS, 449, 820
- Wright, E. L., Eisenhardt, P. R. M., Mainzer, A. K., et al., 2010, AJ, 140, 1868
- Zahid, H. J., Geller, M. J., Kewley, L. J., et al. 2013, ApJ, 771, L19